Development of freeze-drying cycle for a peptide-based drug in trays

Proceedings of Eurodrying'2019
Torino, Italy, July 10-12, 2019

Paper 144

DEVELOPMENT OF FREEZE-DRYING CYCLE FOR A PEPTIDE-BASED DRUG IN TRAYS

***Fiora Artusio*[1], *Andrea Borgogno*[2], *Walter Cabri*[2], *Antonio Ricci*[2], *Claudia Udrescu*[1], *Angelo Viola*[2], *Roberto Pisano*[1]**

[1]Department of Applied Science and Technology, Politecnico di Torino
Corso duca degli Abruzzi 24, 10129 Torino, Italy
E-mail: roberto.pisano@polito.it
[2]Fresenius Kabi iPSUM Srl
Via San Leonardo 23, 45010 Villadose (RO), Italy

Abstract
Freeze-drying of a peptide solution is here presented, from the early identification of critical product temperature to the design of an appropriate cycle. Synergy between experimental characterisation techniques, mathematical modelling and process simulation has been implemented to develop a robust lyophilisation process and guarantee the removal of solvents impurities. Process has been carried out in bulk using a tray equipped with an anisotropic membrane, enabling unidirectional vapour flow.

***Keywords**:* freeze-drying, peptide, mathematical modelling, process simulation

1. Introduction

Lyophilisation provides a useful tool for removing solvents from a product in the perspective of downstream processes and/or preservation of stability and enhancement of product shelf-life. In this scenario, it represents a reliable separation technique which is convenient to purification purposes, such as those linked to the recovery of a final product from water and solvent impurities deriving from early stages of a novel molecule synthesis.

In a typical process, freezing of solution is followed by two drying steps. Primary drying involves the sublimation of frozen solvent, whereas secondary drying is responsible for the removal of unfrozen, thus adsorbed, solvent residues. When a novel or unknown molecule formulation has to be lyophilised, critical product temperatures must be identified, as they represent one of the most relevant process constraints. Other issues regard proper cake formation during drying, avoidance of choked flow to condenser, lyophilised product quality, *etc.* (Hardwick *et al.*, 2008).

In the present study, lyophilisation was employed for recovering a peptide from water and organic solvents impurities. When developing a new freeze-drying cycle, several factors have to be taken into account ranging from formulation to freezing and drying recipes. A Quality by Design (QbD) approach (Pisano *et al.*, 2012) is here applied in order to identify proper process conditions starting from the thermal characterisation of a peptide solution and of its container. Design space (Fissore *et al.*, 2011) was calculated in order to disclose the relationship between safe operating conditions, in terms of chamber pressure and shelf temperature, and temperature of the product during drying. Freeze-drying has been carried out in bulk using a tray equipped with a special membrane enabling unidirectional vapour transport from product to chamber. At the same time, preservation of the product during unloading of freeze-dryer chamber is guaranteed.

2. Material and method

A 50 g/L aqueous solution of peptide, containing 0.3 wt% of acetonitrile and 0.1 wt% of acetic acid referred to peptide, is here investigated. All the operations involving dry product reconstitution were

carried out inside a laminar flow hood in order to avoid contamination. In order to preserve the peptide activity, particular care was taken while preparing the solution by cooling down the solution by means of a cryostat.

Differential Scanning Calorimetry (DSC Q200, TA Instruments, New Castle, DE, USA) was used to investigate thermal behaviour of the peptide solution. A given aliquot of solution (approx. 40 mg) has been loaded in an aluminium container (TZERO pan) and placed in the DSC cell. Nitrogen flow equal to 50 ml/min was ensured throughout the whole analysis. Samples were cooled down from 20 °C to -80 °C at 1 °C/min, kept at -80 °C for 1 min and then heated at 5 °C/min up to 40 °C.

Freeze-Drying Microscope (FDM, microscope: BX51, Olympus Europa, Hamburg, Germany; temperature controller: PE95-T95, Linkam, Scientific Instruments, Tadworth, Surrey, UK) was used to study lyophilisation behaviour of the peptide solution and identify critical temperatures leading to collapse phenomena. Freezing ramp was set at 1 °C/min to -50 °C; lyophilisation occurred at 0.1 mbar while increasing temperature. Two different heating programmes were implemented. For the first cycle, heating occurred at 2 °C/min from -50 °C to -13 °C and at 1 °C/min to 0 °C. The second sample was processed at 2 °C/min from -50 °C to -10 °C and then heating ramp was reduced to 0.2 °C/min in order to increase accuracy in critical temperature determination.

The peptide solution was lyophilised in a lab-scale freeze-dryer (Lyobeta, Telstar, Barcelona, Spain) using a proprietary set-up made of a tray equipped with an anisotropic membrane. This configuration enables unidirectional vapour flow during freeze-drying and, at the same time, preserves the final product during chamber unloading. Pressure control inside freeze-drying chamber was guaranteed by Baratron sensor coupled to "controlled leakage" strategy, which involved manipulation of nitrogen flux introduced into the chamber to maintain the desired degree of vacuum.

Final content of water, acetonitrile and acetic acid residues were determined by means of Karl Fisher titration (CA-31 Moisture Meter, Mitsubishi Chemical Analytech, Kanagawa, Japan), HPLC (Agilent 1260 Infinity II, UV Detector, Agilent Technologies, Santa Clara, CA, USA) and gas chromatography (Agilent 6850, FID Detector, Agilent Technologies, Santa Clara, CA, USA) respectively.

3. Results and discussion

The present study is intended for the development of an efficient freeze-drying cycle for downstream purposes. The main goal is to isolate, purify and recover the peptide after the synthesis, ensuring preservation of activity.

Firstly, thermal characterisation of the reconstituted peptide has been performed, as shown in Fig. 1. DSC analyses pointed out the presence of a glass transition temperature occurring at approx. -8 °C, detected at inflection point. Then, a strong endothermic peak denoted the melting of ice.

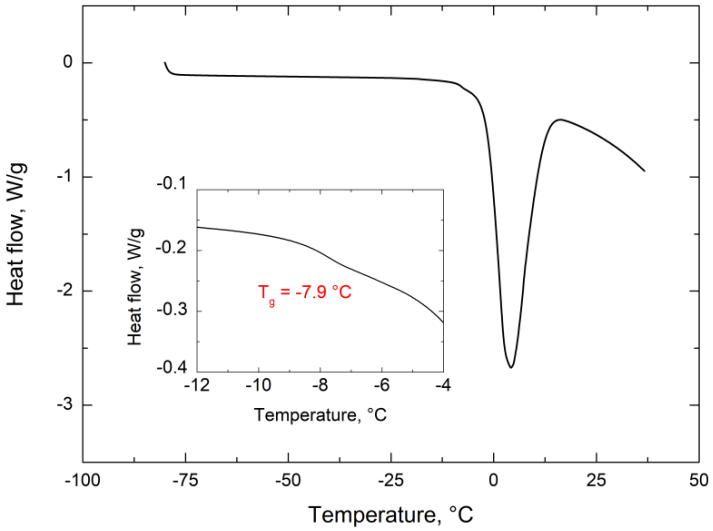

Figure 1. DSC thermogram of peptide solution. Glass transition occurred around -8 °C, as highlighted in the insight.

Structural stability of the peptide solution being lyophilised was then assessed by means of FDM. A first coarse scan involving a fast heating ramp was carried out in order to identify the temperature range in which collapse phenomena occurred. Then, a finer investigation characterised by a much slower heating ramp when approaching coarse critical temperature was performed. As can be seen in Fig. 2, droplet freeze-drying proceeded without structural variations up to -7.9 °C, when the onset of micro-collapse phenomena was detected. Then, macro-collapse of the dried cake occurred at -7.4 °C and degenerated in cake cracking. Such a behaviour was an expected one, as product collapse typically occurs few degrees above glass transition temperature. Since the cake structural stability was remarkably robust, we found out that the peptide solution could be actually lyophilised as it was. Addition of excipients acting as bulking agents for cake creation could thus be avoided.

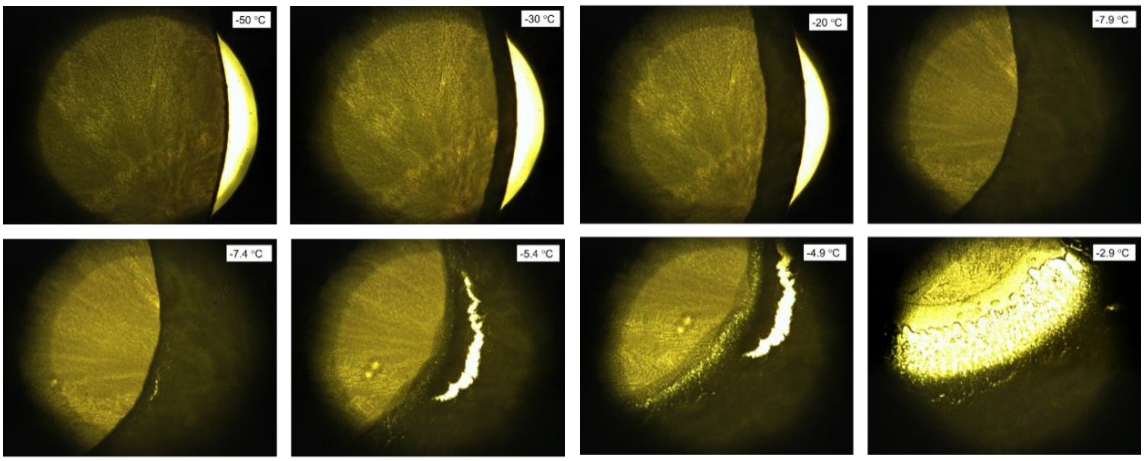

Figure 2. Freeze-drying behaviour of peptide solution as highlighted by FDM.

Therefore, thermal characterisation of the solution enabled us to set the maximum allowable product temperature T_{max}, that is to say the threshold value of the product temperature that must not be overcome during freeze-drying cycle. Taking into account safety margins, this was set at -10 °C and served as reference for the successive design and choice of process operating conditions.

In order to build the Design Space (DS) via mathematical modelling, it is necessary to describe the heat transfer and vapour flow trends (Rambhatla *et al.*, 2004, Pisano *et al.*, 2011) of our proprietary tray and solution. As first step, we focused on the investigation of the thermal behaviour of the tray. The overall heat transfer coefficient, K_v, and its pressure dependence have been determined via gravimetric tests. The tray was loaded with a known amount of water and partial drying was carried out at different chamber pressures (P_c), namely 5, 10 and 25 Pa. In this way, essential information for the modelling of K_v as a function of pressure could have been collected:

$$K_v = a_{Kv} + \frac{b_{Kv} P_c}{1 + c_{Kv} P_c} \quad (1)$$

Model parameters were obtained by fitting of experimental data. For the tray used in this study, the model parameters are listed in Tab. 1. Noticeably, in the range of explored pressures, K_v vs. P_c trend resulted to be almost linear, as reported in Fig. 2a. This meant that heat exchange was significantly influenced by chamber pressure.

Then, an exploratory freeze-drying cycle of the peptide solution was carried out in order to evaluate the resistance of product to vapour mass transfer R_p from regression of experimental data. R_p was modelled as a function of the thickness of the dried product, as highlighted in equation (2) and reported in Fig. 2b:

$$R_p = R_{p0} + \frac{A_{Rp} L_d}{1 + B_{Rp} L_d} \quad (2)$$

The values of the model parameters are listed in Tab. 2. In addition, this methodology enabled determination of the contribution to mass transport resistance provided by the membrane, which

affects R_{p0}, that is to say the resistance to vapour flow at the beginning of drying, corresponding to $L_d = 0$.

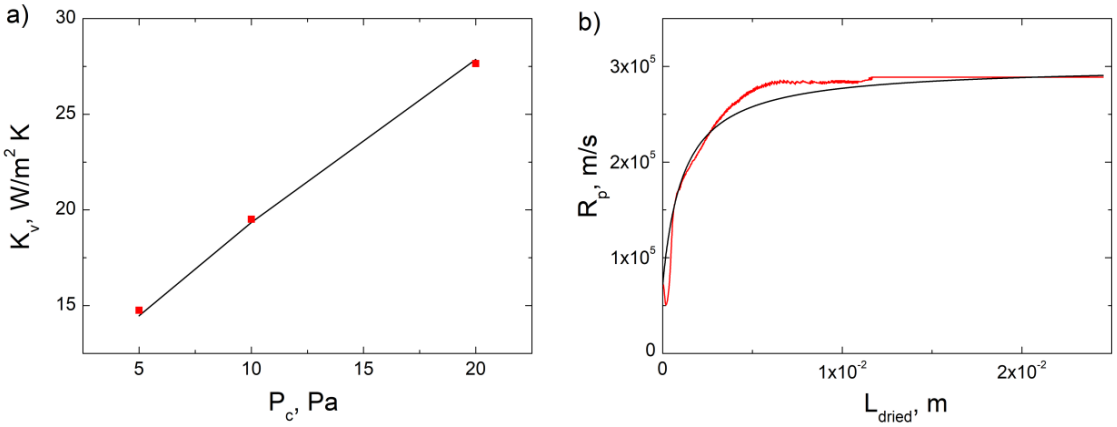

Figure 2. a) K_v vs. P_c for tray processed in the laboratory equipment, (symbols) experimental values and (solid line) model predictions. b) R_p vs. L_{dried} as experimentally observed (red curve) and predicted by the model (black curve).

Table 1. Parameters of K_v and R_p obtained from regression of experimental data.

K_v		R_p	
Parameter	**Value**	**Parameter**	**Value**
a_{Kv}	9.2 W m^{-2}K^{-1}	R_{p0}	7.18×10^4 m s^{-1}
b_{Kv}	113.8 W m^{-2}K^{-1}mbar^{-1}	A_{Rp}	1.92×10^8 s^{-1}
c_{Kv}	1.1 mbar^{-1}	B_{Rp}	865 m^{-1}

Thanks to the preliminary heat transfer characterisation of the tray and vapour transfer resistance of the solution, DS could have been calculated. We ran simulations setting different maximum temperatures of the product, as reported in Fig. 3a, in order to highlight the relationship between allowable process conditions and T_{max}. Design space is time-dependent since a set of operating conditions may be allowable at a certain time t, which corresponds to a specific L_d, and may not belong to DS anymore at another time instant. As a matter of fact, the same set of T_s and P_c can lead to different values of product temperature during drying, as L_d (and hence R_p) varies as long as drying proceeds. Therefore, we decided to refer DS calculation at $L_d = L_{tot}$, where L_{tot} represents the total product thickness, and, thus, to the end of primary drying. In this way, the reported process conditions will belong to DS at every time instant of drying. As can be seen, lowering the threshold temperature value restricts admissible working area in terms of shelf temperature (T_s) and chamber pressure (P_c). However, in our case, as we set T_{max} = -10 °C, the constraints on freeze-drying operating conditions resulted to be less strict. Shelf temperature was truly limited only when dealing with very low degrees of vacuum. Therefore, thanks to our QbD approach, we were able to select quite aggressive, but still safe, processing conditions for primary drying.

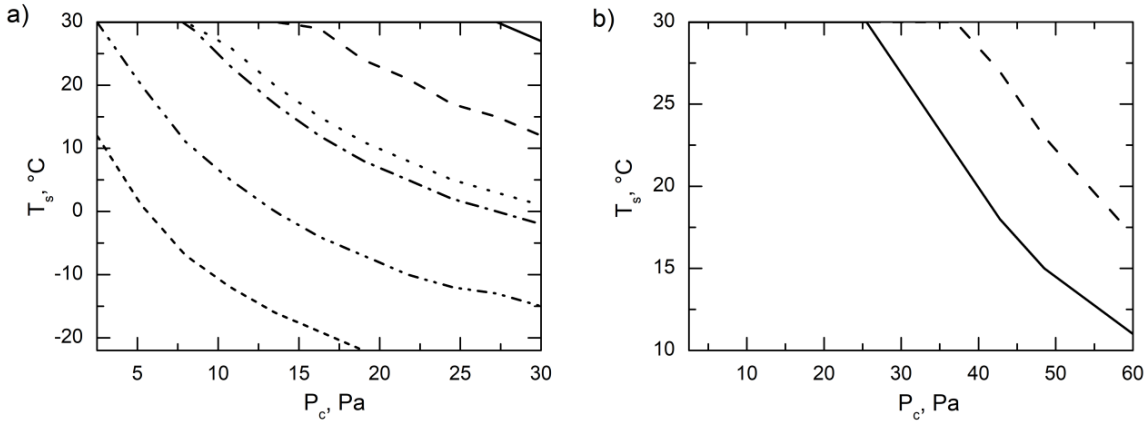

Figure 3. a) Design space for various values of T_{max}:(solid)) -10 °C, (dash) -15 °C, (dot) -19 °C, (dash-dot) -20 °C, (dash-dot-dot) -25 °C, (short dash) -30 °C. b) Design space calculated at T_{max} = -10 °C with (solid) and without (dash) membrane.

The selection of an appropriate combination of chamber pressure and shelf temperature was also based on the outcomes of the process simulation, calculated thanks to preliminary mathematical modelling of freeze-drying behaviour of the system. Primary drying time has been simulated, as well as maximum temperature reached by the product during drying. Simulations were carried out considering different temperatures and pressures for drying. The freezing step was unmodified, and the initial sublimating front temperature was kept constant and equal to -40 °C. Moreover, the contribution of the membrane to the resistance to vapour flow has been evaluated by comparing drying times and product temperatures with and without membrane. The latter case was implemented by setting $R_{p0} \approx 0$, as the contribution to resistance to mass transfer offered by the membrane is supposed to largely overcome that of freeze-dryer chamber. Results are summarized in Tab. 2.

It turned out that the additional resistance provided by the membrane increased the drying time of approx. 10 % and increased product temperature of approx. 5 to 13 % depending on process conditions. As a matter of fact, the removal of membrane results in increased sublimation flux of ice during drying, thus keeping the product at lower temperatures and shortening time needed for drying to be completed. This was corroborated by comparison with DS calculation setting T_{max} = -10 °C and considering the presence or absence of the membrane, as shown in Fig. 3b. When membrane was absent, DS resulted to be significantly broader. However, we demonstrated that this aspect had a marginal impact on process efficiency. Considering the beneficial effects rising from product conservation and protection from humidity during chamber unloading, this would not justify membrane removal.

Table 2. Drying times and product temperatures as emerged from process simulation.

		With membrane		**Without membrane**	
Chamber pressure, Pa	**Shelf temperature, °C**	**Drying time, h**	**Product temperature, °C**	**Drying time, h**	**Product temperature, °C**
10	-10	46.4	-26.8	42.6	-28.3
10	0	33.3	-23.4	31.0	-25.2
10	10	25.7	-20.3	24.1	-22.3
10	20	20.8	-17.4	19.7	-19.6
20	-10	40.0	-23.5	36.6	-24.8
20	20	16.3	-12.9	15.4	-14.8

Our preliminary evaluation of the process enabled considerable savings of time and experimental work thanks to the synergy between mathematical modelling and predictive process simulation. In this frame, we designed a freeze-drying cycle in order to guarantee two main quality constraints. Product temperature must be below T_{max} and, at the same time, water and organic solvents must be removed.

To achieve this goal, a freeze-drying cycle has been performed on our laboratory-scale equipment. The freezing protocol involved approx. 3 hours of ramp and 2 hours of holding at -40 °C. Both primary and secondary drying were carried out at the same shelf temperature and chamber pressure, i.e. at 20 °C and 20 Pa respectively. This choice emerged from our previous process simulations, which highlighted that such a combination of operating conditions would guarantee short drying times, around 20 h, and acceptable product temperature during drying. As regards the operating conditions selected for secondary drying, shelf temperature and time were set at 20 °C and 18 h. The former represented a compromise between favouring desorption kinetics of solvents and avoiding potential denaturation of the peptide. The latter ensured meeting of final specifications on residual moisture, acetonitrile and acetic acid with a large safety margin. Effective processing conditions and length of the various steps are reported in Tab. 3, whereas Tab. 4 collects the residual solvent contents for the lyophilised product.

Table 3. The operating conditions of freeze-drying cycle.

Step	**Shelf temperature, °C**	**Chamber pressure, Pa**	**Time, h**	**Product temperature, °C**
Freezing	-40	amb.	5	-38
Primary drying	20	20	25	-17
Secondary drying	20	20	18	22

Table 4. Residual moisture, acetonitrile and acetic acid contents after freeze-drying.

	Freeze-dried product	**Final specification**
Water content, %	5.2	≤ 8
Acetonitrile, ppm	124	≤ 410
Acetic acid, %	10.0	7.6 – 12.8

As can be noticed, real drying time and product temperature were in good agreement with the model predictions, confirming reliability of our mathematical model. The total duration of the cycle was within 48 h, thus meeting large-scale production requirements. Furthermore, we achieved small residual moisture and drastically reduced acetonitrile and acetic acid contents. As the latter represents the source of counterions for the peptide, it turned out that the residual acetic acid content was very close to the stoichiometric one.

A final remark regards cycle robustness. Safety margins referring to chamber pressure (χ_P) and shelf temperature (χ_T) were calculated at different time intervals of drying and have been referred to the normalized length of dried product (Fissore *et al.*, 2012). As can be seen in Fig. 4, as long as drying proceeds, DS becomes more and more restrictive and both safety margins progressively decrease. However, in the worst scenario, i.e. at the end of drying, maximum allowable fluctuations in pressure and temperature would be 20 Pa and 10 °C, as outlined in Tab. 5. Such an estimation corroborates our cycle robustness by giving a quantitative indication of accepted deviations of operating conditions.

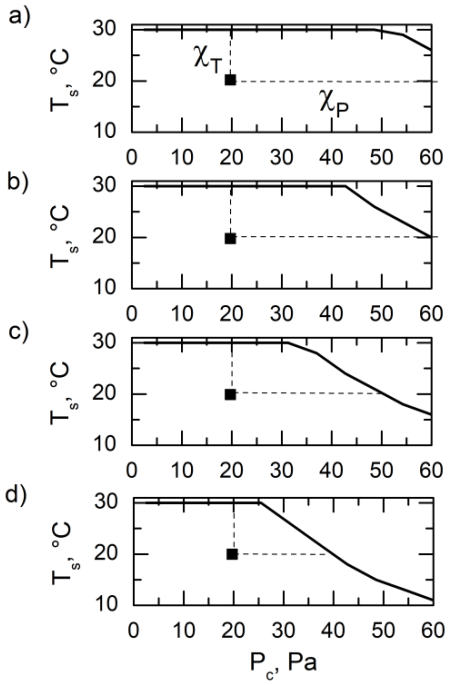

Figure 4. DS as calculated considering various values of L_{dried}/L_{TOT}: a) 1 %, b) 12 %, c) 23 % and d) 99 %.

Table 5. Safety margins for shelf temperature and chamber pressure as emerged from DS.

L_{dried}/L_{tog}	χ_T, °C	χ_P, Pa
1 %	10	> 40
12 %	10	40
23 %	10	30
99 %	10	20

4. Conclusions

The present study was intended for the development of a freeze-drying cycle involving a solution of peptide-based drug. The characteristic temperature of the solution was determined by DSC and FDM and served as reference for the design of an appropriate lyophilisation cycle. Proper cake formation of our peptide solution was confirmed by means of FDM and this avoided the addition of excipients. Heat exchange coefficients of our proprietary tray have been modelled as a function of pressure. Then, the freeze-drying behaviour of the reconstituted peptide has been modelled in terms of resistance to vapour flow. These two aspects were pivotal to the calculation of DS and process simulation. Operating conditions of drying were carefully tailored in order to guarantee final product quality, minimise drying time and ensuring a robust freeze-drying cycle. Safety margins have been evaluated in terms of allowable fluctuations in chamber pressure and shelf temperature during primary drying. The additional mass transfer resistance offered by the membrane was evaluated too and resulted to be marginal. Our optimised cycle enabled removal of water and other solvents impurities and cycle scale-up is currently being studied. In conclusion, synergy between experimental and modelling techniques enabled the development of an optimised and safe freeze-drying cycle at lab-scale and will support scale-up for mass production.

References

Fissore D., Pisano R., Barresi A. A., 2011, Advanced approach to build the design space for the primary drying of a pharmaceutical freeze-drying process, *J. Pharm. Sci.* **100**(11), 4922-4933.

Fissore D., Pisano R., Barresi A. A., 2012, A model-based framework to optimize pharmaceuticals freeze-drying, *Dry. Technol.* **30**(9), 946-958.

Hardwick L. M., Paunicka C., Akers M. J., 2008, Critical factors in the design and optimization of lyophilisation processes, *Innovations Pharm. Technol.* **26**, 70–74.

Pisano R., Fissore D., Barresi A. A., 2011, Heat transfer in freeze-drying apparatus., in *"Heat Transfer"* (Dos Santos Bernardes, M. A., Ed.), InTech, Rijeka, Croatia, pp. 91-114.

Pisano R., Fissore D., Barresi A. A., Brayard P., Chouvenc P., Woinet B., 2012, Quality by design: optimization of a freeze-drying cycle via design space in case of heterogeneous drying behavior and influence of the freezing protocol, *Pharm. Dev. Technol.* **18**(1), 280-295.

Rambhatla S., Ramot R., Bhugra C., Pikal M. J., 2004, Heat and mass transfer scale-up issues during freeze drying: II. Control and characterization of the degree of supercooling, *AAPS PharmSciTech*., **5**(4), Article no. 58.